Supporting Information

4D Printed Transformable Tube Array for High-throughput 3D Cell Culture and Histology

Chen Yang, Jeffrey Luo, Marianne Polunas, Nikola Bosnjak, Sy-Tsong Dean Chueng, Michelle Chadwick, Hatem E. Sabaawy, Shawn A. Chester, Ki-Bum Lee and Howon Lee**

Materials

All chemicals including both liquid oligomers, photoinitiator (PI), and photo absorber (PA) were purchased from Sigma-Aldrich (St. Louis, MO, USA) and used as received. Poly(ethylene glycol) diacrylate (PEGDA) (Mn 250) and Bisphenol A ethoxylate dimethacrylate (BPA) (Mn 1700) were mixed at a ratio of 9:1 in weight. Phenylbis(2,4,6-trimethylbenzoyl) phosphine and Sudan I were added additionally at a concentration of 2 wt.% and 0.1 wt.% of the precursor solution as PI and PA, respectively.

Composition of shape memory polymer

The weight ratio of PEGDA250 and BPA was investigated to determine a copolymer blend with an effective T_g around 60 ºC. The T_g of PEGDA250 was reported as 65 ºC[1] and the T_g of BPA was reported as -40 ºC[2]. The effective T_g of a copolymer system can be estimated using Gordon-Taylor equation[3]

$$T_g = \frac{w_1 T_{g1} + k w_2 T_{g2}}{w_1 + k w_2}, \quad (1)$$

where T_g, T_{g1} and T_{g2} are the glass transition temperature of the copolymer, PEGDA250 and BPA, respectively. w_1 and w_2 are the weight percentage of PEGDA250 and BPA in the copolymer, and $k = 0.36$ is an empirical factor evaluated from the experiment. T_g of different weight ratios between PEGDA250:BPA were plotted in **Figure S1**. A PEGDA250:BPA weight ratio of 9:1 was chosen, whose T_g was estimated to be 61 ºC. From the DMA result in **Figure 2a**, the actual copolymer had a glass transition temperature of 60 ºC.

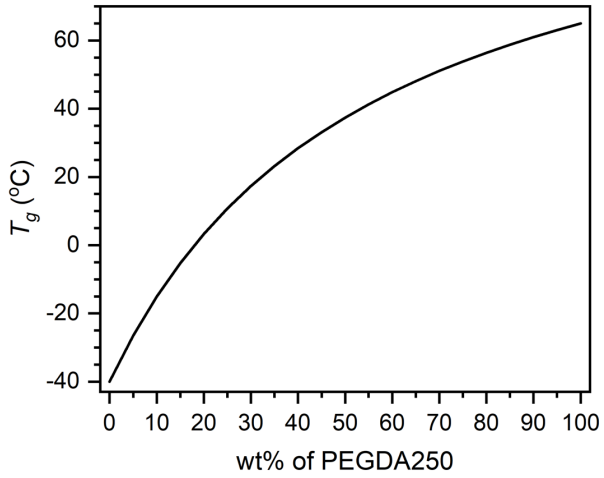

Figure S1. T_g estimation of SMP as a function of PEGDA250 wt% using Eq. (1).

Projection micro-stereolithography (PμSL)

A custom-built PμSL system was used in this work. It consists of a UV LED (365 nm) (L10561, Hamamatsu), a collimating lens (LBF254-150, Thorlabs), a digital micro-mirror device (DMD^{TM}) (DLPLCR6500EVM, Texas Instruments), three motorized linear stages (MTS50-Z8, Thorlabs), and a projection lens (Thorlabs). The entire PμSL system was kept in a UV blocking enclosure. In the fabrication process, the 3D computer-aided-design (CAD) model was first discretized into 2D images. These images were fed one-by-one to a customized digital light projector (DLP) projector to create solid layers of precursor solution until finished. The resolution of the digital micromirror device (DMD) in the PμSL system is 1920 pixel x 1080 pixel, and one projection area is 24 mm x 14 mm, making the nominal resolution 13 μm/pixel. To print the TTA with dimensions of 30 mm x 20 mm x 11 mm, we divided each layer to 3 by 2 projections with 800-pixel x 800-pixel (~10 mm x 10 mm) areas utilizing horizontal XY stage movement. Printing parameters used were light intensity of 29 mW cm^{-2}, a layer thickness of 50 μm, and curing time of 1 sec/layer.

Post-processing

Printed samples were rinsed in fresh ethanol for 30 sec for 4 times to remove uncured precursor solution. After rinsing, the samples were air-dried until the absorbed ethanol evaporated. The samples were then rinsed in pentane one more time to avoid capillary-driven adhesion between helical arms and neighboring tubes. After the pentane evaporated, the samples were post-cured in a UV oven (CL-1000L, UVP, 365 nm) for 1 hour from the top and 1 hour from the bottom to fully crosslink the sample. To remove cytotoxic residual materials, a series of soaking steps were given using an ultrasonic cleaner (360HTD, Preup): at 50 ºC, sonication in 100 mL acetone for 1 hour; at 50 ºC, sonication in fresh 100 mL acetone for 1 hour and soaking for 11 hours; at 60 ºC, sonication in fresh 100 mL hexane for 1 hour and soaked for 11 hours. Sonication and soaking steps with acetone and hexane were repeated one more time to finish the soaking process. Afterward, the soaked samples were dried in a vacuum oven at 700 mmHg vacuum and 80 ºC for 2 hours. Before cell seeding, the TTA was sanitized using ethanol and 15 min UV exposure. Then the samples were dried in a fume hood overnight at room temperature.

Mold casting

SMP samples for mechanical testing were prepared using mold casting. Glass slides were cleaned with ethanol and coated with RainX for easy demolding. The SMP precursor solution without PA was injected in a mold of two glass slides separated by 0.15 mm spacers. An SMP sample was cured in a UV oven with a light intensity of 5 mW cm^{-2} for 20 min on each side, yielding a fully cross-linked polymer film with a thickness of 0.15 mm. Samples were then laser cut to 30 mm x 1 mm x 0.15 mm rectangular specimens.

Dynamic mechanical analysis (DMA)

Samples were 3D printed with the same printing parameters and post-processing procedures (except sanitization steps). Dimensions of 3D printed samples were 25 mm x 6 mm x 0.15 mm. DMA was conducted on a dynamic mechanical analyzer (DMA850, TA Instruments) using film tension clamps. Testing parameters for DMA included a strain of 0.2 %, frequency of 1 Hz, preload of 0.005 N, and force track of 150 %. Specimens were heated at 25 °C for 10 min prior to the test. Storage modulus, loss modulus, and tanδ were measured as a function of temperature while the temperature was increased from 25 °C to 75 °C at a rate of 1 °C min^{-1}.

Effect of swelling on the glass transition temperature of SMP

It has been reported that water absorption decreases the T_g of an SMP.[4,5] During cell culture, helical arms, which oversees the shape recovery, are not fully immersed in the aqueous culture media, but diffusion from the immersed cell chambers can still affect the T_g of the SMP. To understand the effect of aqueous solution exposure, DMA of the same SMP was conducted while fully immersed in water. DMA test in water used submersion film tension clamps. 3D printed samples were 15 mm x 6 mm x 0.15 mm. Testing parameters were kept the same except for a temperature range of 20 °C to 65 °C. DMA tests performed in an aqueous environment show that swelling decreases T_g of the SMP from 60 °C to 31 °C (**Figure S2**), which is below the cell incubation temperature. Since the TTA loses its ability to hold the stretched geometry when in contact with culture media during culture, we created a fixture as shown in **Figure S7** to fix the TTA in place on a 96-well plate during the culture period.

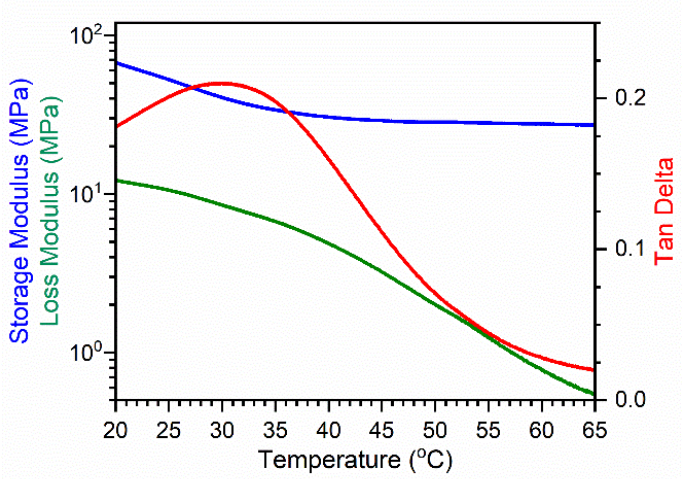

Figure S2. DMA results of the SMP immersed in water.

Shape memory cycle

A mold-casted sample was first heated to 60 °C. At 60 °C, the specimen was stretched to 8% of strain a strain rate of 0.1 % sec^{-1}. After maintaining the strain constant for 10 min at 60 °C, the temperature was decreased to 25 °C and the strain was kept constant for another 10 min. Loading was then released, and the remaining strain at 25 °C was measured 10 min after the load was removed. The shape-fixity ratio was calculated using $\varepsilon_1/\varepsilon_0$, where ε_0 is the total strain of stretching and ε_1 is the strain that remained 10 min after stress was released. Upon heating back to 60 °C, the strain of the SMP decreased. The shape-recovery ratio was calculated using $1-\varepsilon_2/\varepsilon_0$, where ε_0 is the total strain of stretching and ε_2 is the strain that remained after shape recovery at 60 °C.

Failure strain test

Dynamic mechanical analyzer with film tension clamps was used to measure strain at failure at different temperatures. A mold-casted sample was kept at the desired temperature for 10 min and then stretched to failure at a strain rate of 0.1 % sec^{-1}. The test was repeated for 3

samples at each temperature. The strain at failure from 3 tests was averaged and plotted in the bar chart with error bars showing maximum and minimum values in the test.

Design of transformable tube array

As shown in **Figure S3a**, the transformable tube array (TTA) was printed in the collapsed configuration with dimensions of 2.5 mm x 2.5 mm x 11 mm, where 8.05 mm was for helical arms and 2.95 mm was for cell chamber. A TTA with 96 cell culture tubes in a 12 x 8 array was 30 mm x 20 mm x 11 mm in the collapsed configuration (**Figure S3b**). The inner diameter of a culture tube was designed to be 1.9 mm to facilitate cell seeding with a 10 μL pipette tip (tip diameter of ~ 1 mm). The cell chamber wall and helical arms thicknesses were both 200 μm. The width of the helical arms was 1.45 mm with a spacing of 0.8 mm. In the design, the TTA consists of culture tubes with alternating clockwise and counterclockwise helical arms. Based on empirical trials, this arrangement reduces helical arm twisting during stretching to a greater extent than a uni-rotational configuration.

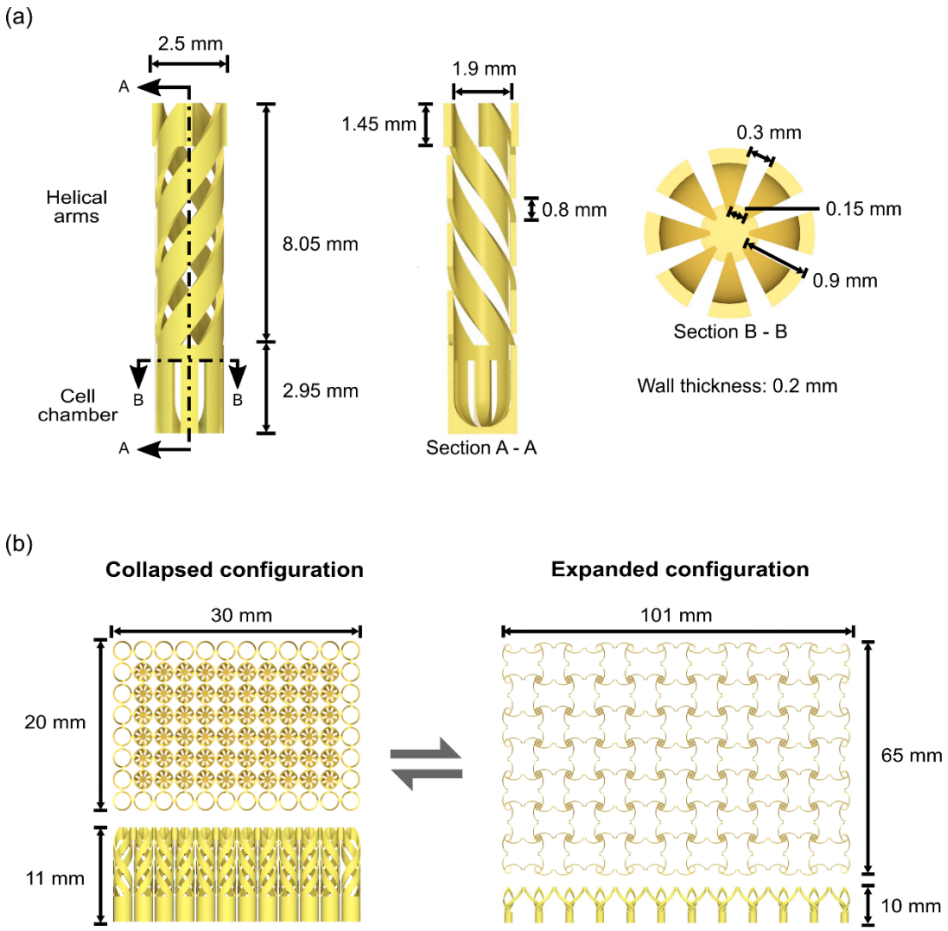

Figure S3. Detailed design of the TTA. (a) Design of the culture tube. (b) Dimensions of the TTA in the collapsed configuration and the expanded configuration.

Finite element simulation

Numerical simulation was performed in the commercially available software package Abaqus/Explicit (Abaqus, 2020. Abaqus Reference Manuals. Dassault Systemes Simulia, Providence, RI.). The polymer in use was modeled utilizing the Abaqus built-in features, more specifically, employing the Neo-Hookean model for the time-independent response, the Prony series for viscoelasticity, and a combination of the Arrhenius-type form[8] and the Williams-Landel-Ferry (WLF) model[9] for the temperature-dependent shift factor.

First, the master-curves in **Figure S4a** were assembled at the glass transition temperature (T_g = 60°C or θ_g = 333 K) by superpositioning the storage and the loss moduli

obtained through DMA at different temperatures and frequencies ω. The frequency-dependent Prony series model was then calibrated against the master-curves to obtain the material parameters. The specific forms for the storage modulus

$$G_S(\omega) = G_0\left[1 - \sum_{i=1}^{10} g_i\right] + G_0 \sum_{i=1}^{10} \frac{g_i \tau_i^2 \omega^2}{1 + \tau_i^2 \omega^2}, \tag{2}$$

and the loss modulus

$$G_L(\omega) = G_0 \sum_{i=1}^{10} \frac{g_i \tau_i \omega}{1 + \tau_i^2 \omega^2}, \tag{3}$$

involve the instantaneous modulus G_0, along with the moduli g_i and relaxation times τ_i for each Prony series *i*. The comparison between the calibrated model and the master-curves is shown in **Figure S4a**, and the calibrated parameters are provided in **Table S1**. The calibrated instantaneous modulus $G_0 = 1.08$ GPa was also used in the Neo-Hookean model, and the material was assumed to be nearly incompressible, thus we took the bulk modulus $K = 10^2\ G_0 = 108$ GPa.

Next, to account for the temperature-dependent shift factor $\mathrm{a_T}$, we calibrated the Arrhenius-type form for the $\mathrm{a_T}$ below the glass transition temperature

$$\ln(\mathrm{a_T}) = \frac{E_0}{R}\left(\frac{1}{\theta - \theta^z} - \frac{1}{\theta_0 - \theta^z}\right), \tag{4}$$

and the WLF model for the $\mathrm{a_T}$ above the glass transition temperature

$$\log(\mathrm{a_T}) = -\frac{C_1(\theta - \theta_0)}{C_2 + (\theta - \theta_0)}. \tag{5}$$

Here, E_0 is the activation energy and $R = 8.3145\ \mathrm{J \cdot K^{-1} mol^{-1}}$ is the universal gas constant. The temperature under consideration θ is given in kelvins, along with the reference temperature $\theta_0 = \theta_g$, and the absolute zero θ^z. Comparison between the calibrated models and the

experimentally observed shift factor is shown in **Figure S4b**, and the calibrated parameters E_0, C_1 and C_2 are provided in **Table S2**.

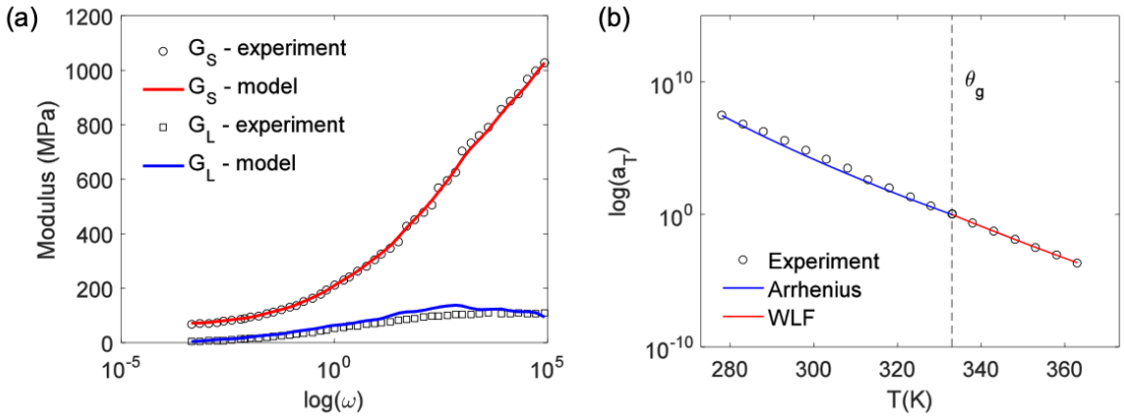

Figure S4. (a) G_S and G_L master-curves assembled at the glass transition temperature. The calibrated Prony series model is plotted on top of the experimental data for comparison. (b) Comparison between the experimentally observed shift factor a_T and the calibrated Arrhenius-type and WLF models.

Table S1. Calibrated moduli and relaxation times for Prony series.

i	g_i	τ_i(s)
1	0.162	$2 \cdot 10^{-5}$
2	0.146	$2 \cdot 10^{-4}$
3	0.152	$1.1 \cdot 10^{-3}$
4	0.113	$4.9 \cdot 10^{-3}$
5	0.127	0.029
6	0.081	0.2
7	0.066	1.18
8	0.044	6.77
9	0.03	49.91
10	0.015	494.65

Table S2. Calibrated WLF and Arrhenius-type form parameters.

WLF parameters	Arrhenius-type form parameter
$C_1 = 57.02$	$E_0 = 2.41 \cdot 10^5\ \mathrm{J} \cdot mol^{-1}$
$C_2 = 441.73$ K	

To simulate the response of a device undergoing mechanical deformation, we meshed a single culture tube using 2183 C3D8T and 337 C3D4T elements. A mechanical displacement u=3.25 mm was prescribed at the connecting surfaces along axis 1 and 3 (the total expansion of the device was 3.6) (**Figure S5**). The bottom surface S was allowed to rotate around the axis 2, while all other mechanical displacements were constrained at this surface. The temperature throughout the simulation was $\theta = 298$ K (T =25°C). For simplicity, the contact between the arms was assumed to be frictionless.

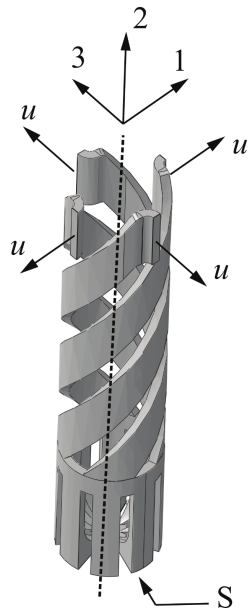

Figure S5. Notations and boundary conditions in finite element simulation.

Biaxial stretching device

The biaxial stretching device was designed as a stack of two circular plates. The top plate had 10 straight rails and the bottom plate had 10 curved rails, as shown in **Figure S6a**. The 10 rails on the top plate connect locations of 10 evenly distributed culture tubes on the perimeter of the TTA in a collapsed configuration to their corresponding locations in the expanded configuration. The curved rails on the bottom plate were designed such that the radial position of the intersections between the top and bottom rails depends on the relative rotational

angle between the two plates. Top rails have a width of 5 mm and bottom rails have a width of 3 mm. The two circular plates with prescribed rails were fabricated with two acrylic plates using a laser cutter. Cylindrical carriers have a diameter of 5 mm in the top portion and 3 mm in bottom portion were inserted at each intersection of the 10 pairs of rails from the top and bottom plates. Each carrier has a needle pin (diameter of 0.8 mm), with which the TTA is engaged. Through rotation of the top plate against the bottom plate, pins radially move outward from the dimension of the cassette configuration (27.5 x 17.5 mm) to the dimension of the 96-well plate configuration (98.5 x 62.5 mm). When the top plate was rotated against the bottom plate, all carriers moved outward, stretching the engaged TTA biaxially from the printed dimension to the expanded configuration. Pictures of the TTA mounted and stretched on the stretching device are shown in **Figure S6b**. The percentage elongation as a function of rotation angle was obtained from the CAD assembly and plotted in **Figure S6c**. This stretching device was capable of a 500% stretch.

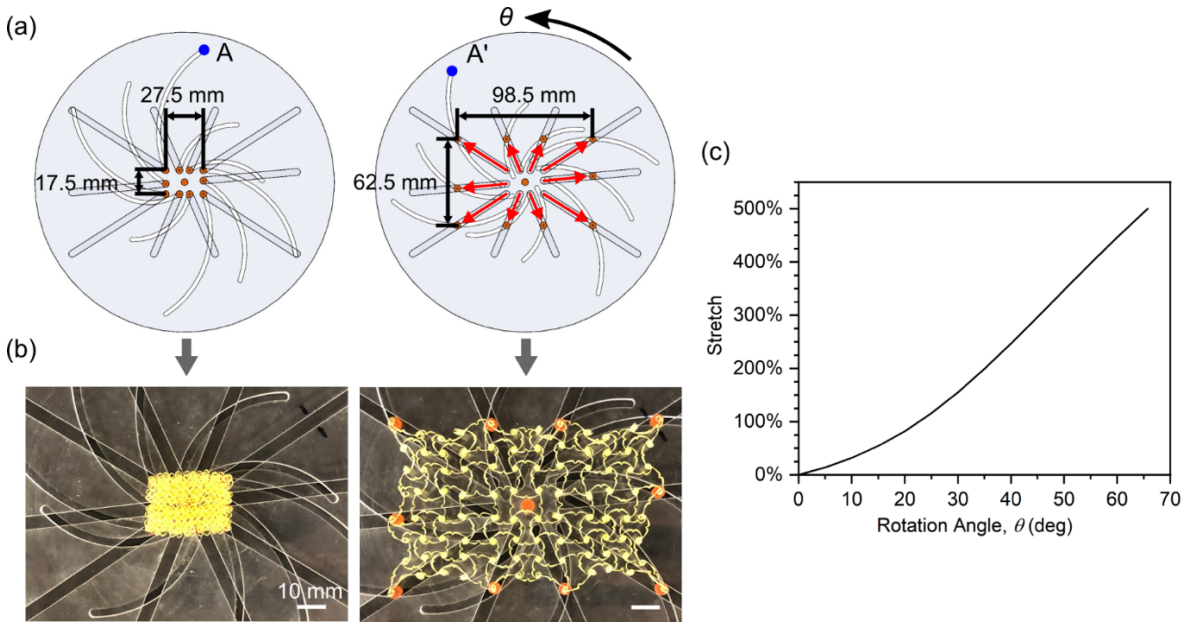

Figure S6. Biaxial stretching device. (a) Design of the stretching device. Points A and A' show counterclockwise rotation of the bottom plate with 10 curved rails, resulting in radial movement of the carriers (red arrows). (b) Biaxial stretching the TTA using the stretching device. Scale bars are 10 mm. (c) Stretch (%) as a function of the rotation angle of the stretching device.

96-well plate fixture

To fix the TTA in place on a 96-well plate during the culture period, we created a fixture with an array of pins as shown in **Figure S7a**. Pins were located at the center of microwells on the perimeter and separated by a distance of 9 mm. The fixture was 3D printed using a fused deposition modeling (FDM) printer (μPrint, Stratasys). CAD design and a picture of the 96-well plate fixture are shown in **Figure S7**. Culture tubes on the outer edge were designed to have an open bottom (**Figure S3b**), so they can be engaged with the pins on the fixture.

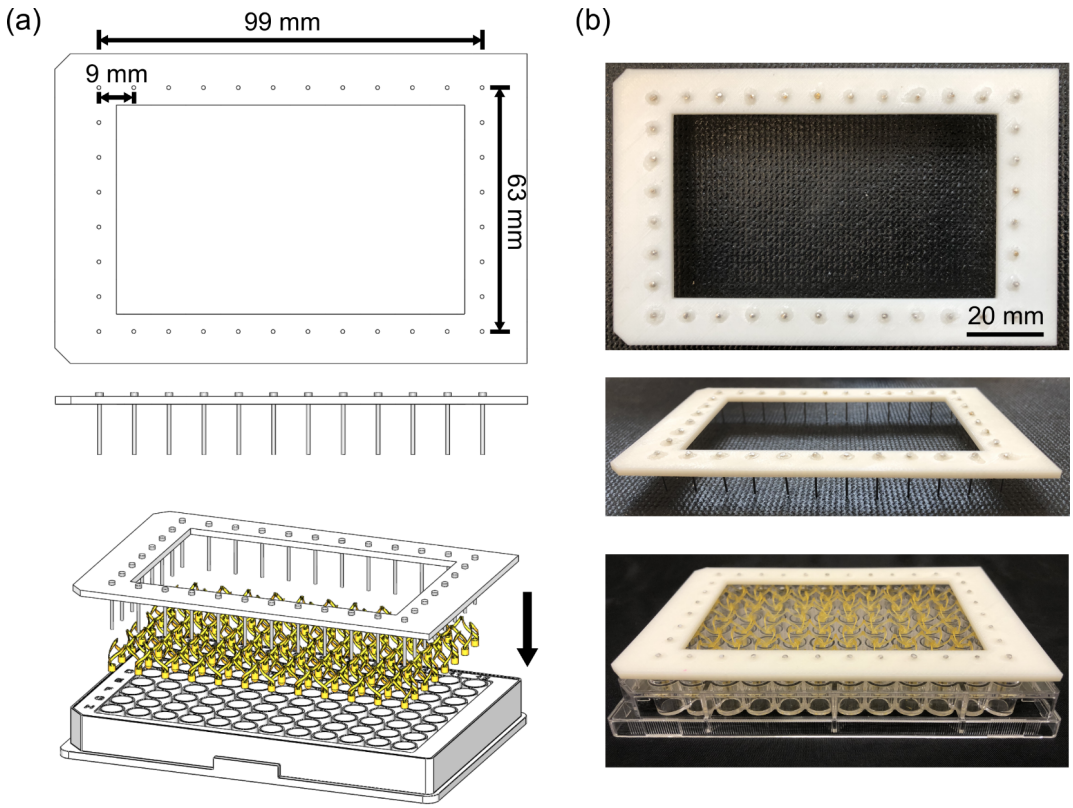

Figure S7. Mounting fixture for TTA. (a) Design of the fixture. (b) TTA mounted on a 96-well plate using the fixture. Scale bar is 20 mm.

Shape programming of the TTA

The TTA was stretched to the expanded configuration at room temperature using the biaxial stretcher. Then, the TTA on the stretcher was placed in an oven at 60 °C for 10 min and

cooled down to room temperature for 10 min for shape fixing. Afterward, the stretched TTA was transferred to a 96-well plate for culture. To evaluate shape programming, a picture of the stretched TTA was taken and overlaid on a drawing of a 96-well plate. The positions of the inner 60 culture tube centers were measured with respect to the centers of their corresponding wells in the 96-well plate.

Shape recovery of the TTA

To recover the original shape, the TTA was first removed from the 96-well plate and heated at 60 ºC for 2 min. A transparent polycarbonate sheet was used as the door of an oven for visibility during the experiment. A 45-degree mirror was set above the TTA in the oven, so a digital camera (Canon 60D) can monitor the top view of the TTA from outside. The temperature inside the oven was set at 60 ºC. The stretched TTA was quickly moved into the oven, and recovery started immediately. After obtaining a video of shape recovery at 30 fps, frames were obtained at specific time points shown as datapoints in **Figure 3f**. The overall length and width of the TTA were measured using ImageJ. Measurements were taken from 6 different locations in the same TTA at each time point, which were then divided by the corresponding number of culture tubes to obtain the average size of one culture tube (D_t) at each time point. D_t was divided by the original printed dimension (D_0). Error bars in **Figure 3f** represent a standard deviation.

Embedding routine for the TTA

A routine was invented for TTA embedding to ensure vertical alignment of culture tubes. After dehydration and paraffin processing in an automated processor (Tissue-Tek VIP, Sakura), the TTA was moved from histology cassette to a large shallow base mold (Tissue-Tek 4123, Sakura). The shallow mold was then filled with liquid paraffin wax and cooled to solidify the

paraffin wax. At this point, paraffin wax covered only the bottom portion of the TTA (above cell chamber). After removing the TTA from the mold, helical arms of the TTA were cut off, and excessive paraffin wax on the side was trimmed. The trimmed block was then placed into a large deep base mold (Tissue-Tek 4132, Sakura) and re-melted. Cell chambers sank to bottom due to gravity, and then more liquid paraffin wax was added to fill the mold. Before the paraffin wax solidified, the mold was capped with a cassette. After cooling, the paraffin block was demolded and ready for sectioning (**Figure S8**).

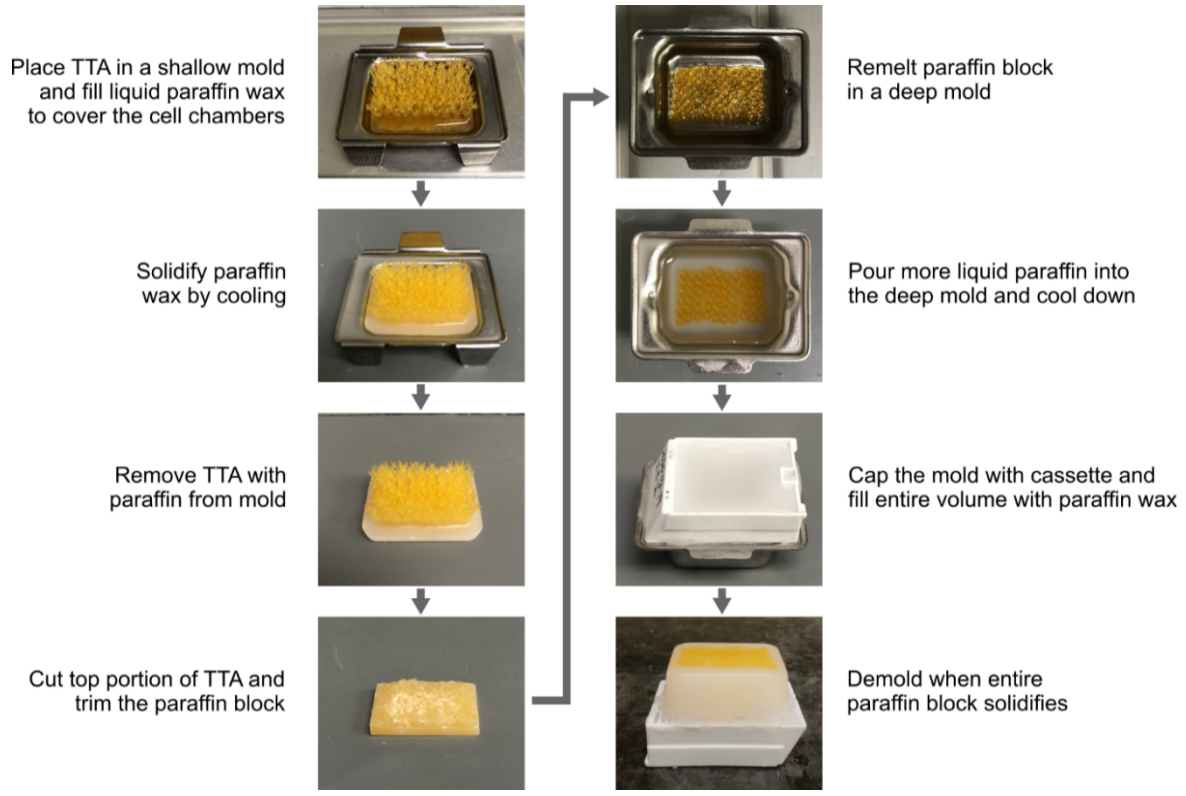

Figure S8. Embedding routine for the TTA.

Characterization of vertical alignment through sectioning

To characterize the vertical alignment of cell chambers in sectioning, we sectioned an embedded TTA from using the embedding routine. Sectioning from the bottom produces snowflake-shaped sections before reaching the inner side of the cell chamber. Once it reaches

the inner chamber, sections show a hollow center. We defined a reference plane when half of the cell chambers show a hollow center. Images of sections at different relative distances are shown in **Figure S9d**.

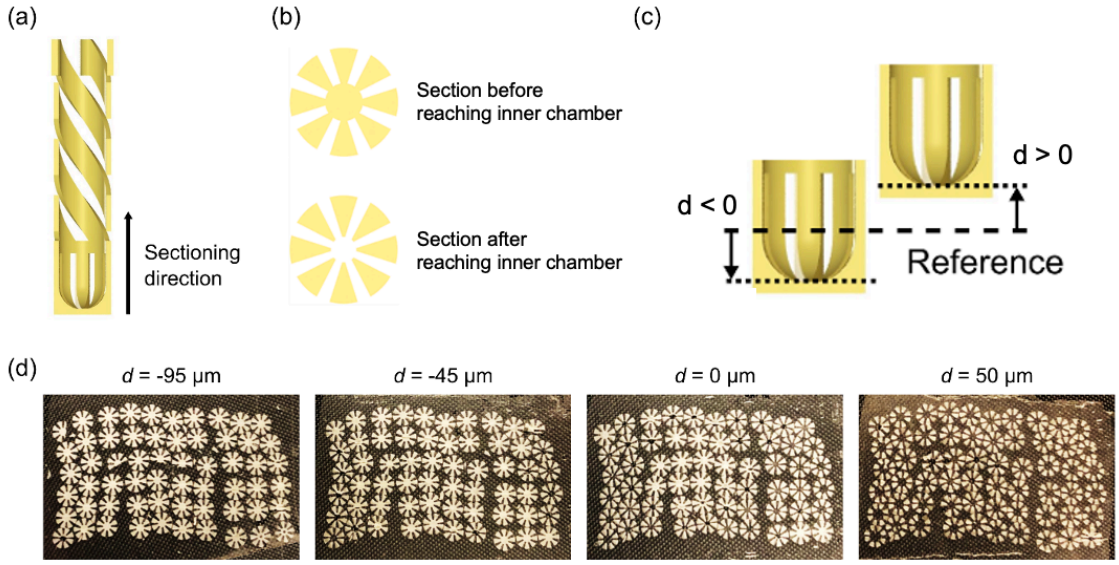

Figure S9. Characterization of vertical alignment through sectioning. (a) Sectioning direction. (b) A snowflake-shape pattern in sections before reaching the inner cell chamber and hollow center in sections after reaching the inner cell chamber. (c) Measuring relative distance from the inner cell chamber bottom to the reference plane. (d) Images of sections at different relative distances.

Reproducibility of TTA performance

The shape programming and recovery of the TTA was very consistent and reproducible in our experiments. To demonstrate the reproducibility of TTA performance, a set of experiments (shape programming, shape recovery, and vertical alignment tests) were conducted with three TTA samples. The results from a total of three samples clearly show the consistent and reproducible performance of the TTA as shown below.

(1) Shape programming

To assess how accurately culture tubes are registered to the corresponding microwells in a 96-well plate after shape programming, we measured the location of each culture tube relative to the center of the microwell using image analysis. As shown in **Figure S10a**, it was consistently observed from all three TTA samples that all of the culture tubes of each TTA consistently fall within the boundary of the corresponding microwells. The result from TTA#1 is presented in the main text as **Figure 3e**.

(2) Shape recovery

To demonstrate that the TTA can transform into its collapsed configuration through temperature-responsive shape recovery, we performed shape recovery tests with three TTA samples at 60 ºC. As shown in **Figure S10b**, we observed that all three TTA samples collapsed consistently at the same rate into a contracted configuration that can be easily placed in a histology cassette. Slight variation among samples was observed due to the difficulty in controlling friction from the surface during shape recovery. The result from TTA#1 is presented in the main text as **Figure 3f**.

(3) Vertical alignment

We evaluated vertical positions of culture tubes when the TTA was embedded into a paraffin block using the embedding routine. Consistent and precise vertical positioning of all culture tubes is important to ensure that all 3D tissue models in the TTA are cut through together into one section. As shown in **Figure S10c**, the sections from all three TTA samples were distributed consistently within 150 μm, confirming the reproducible performance of the TTA. The result from TTA#1 is presented in the main text as **Figure 3g**.

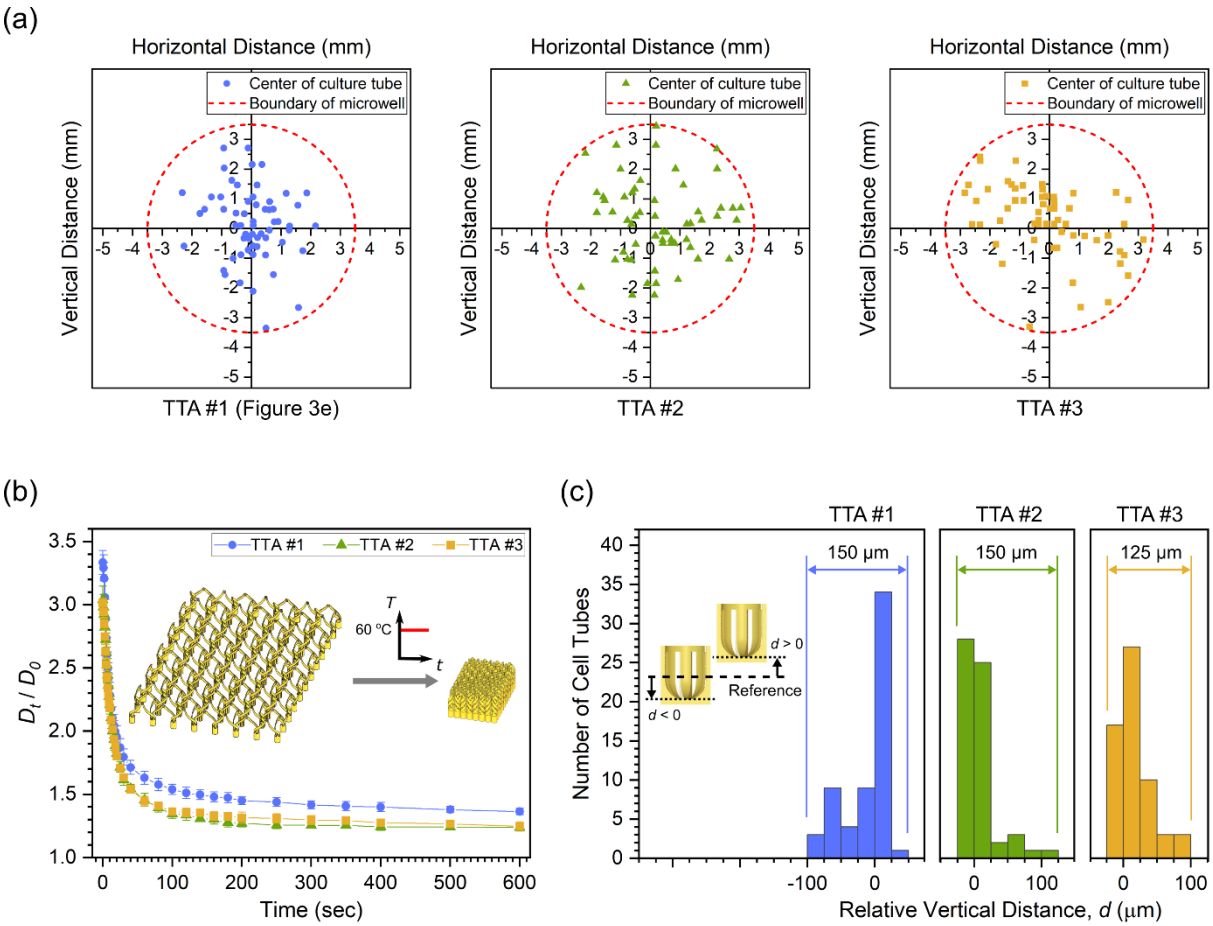

Figure S10. Reproducibility of TTA performance. (a) Positions of the center of culture tubes relative to corresponding microwells in the stretched state. (b) Shape recovery of the TTA upon heating at 60 °C. (c) Distribution of relative vertical positions of cell chambers from a reference sectioning plane.

Parallel processing with a TTA

A proof-of-concept experiment with two dyed polymers is shown in **Figure S11**. A TTA (without slits) in the collapsed configuration was first stretched to the expanded configuration at room temperature. After placing the TTA on the stretching device in the oven at 60 °C for 10 min and cooling back to room temperature, the TTA was removed from the stretching device and mounted on a 96-well plate. The same SMP precursor solution without photo absorber was labeled with Rhodamine B (λ_{ex}=540, λ_{em}=625 nm; magenta in the fluorescent microscope

image. Red signal from Rhodamine B was replaced with magenta in the fluorescent microscope image for readers with red-green color-blindness) or DiOC2 (λ_{ex}=482, λ_{em}=497 nm; green in the fluorescent microscope image), injected into cell chambers in an alternating pattern, and cured with UV exposure. The TTA was then brought back to the cassette configuration by heated shape recovery and placed into a histology cassette. The sample underwent processing in the tissue processor and was embedded in paraffin wax using the same steps as biological samples. Sectioning on a microtome was performed with 10 µm slices. Sections were collected in a warm water bath and then transferred to glass slides. Images from the fluorescence microscopy showing alternating colors demonstrated the result of parallel histological processing. Note that the ruptures were artifacts caused by cutting the rigid solid polymer into thin slices of disks having a large aspect ratio (disk diameter: 2.3 mm, thickness: 10 µm). These ruptures were not observed in the sections of typical TTAs used for regular biological tissue processing.

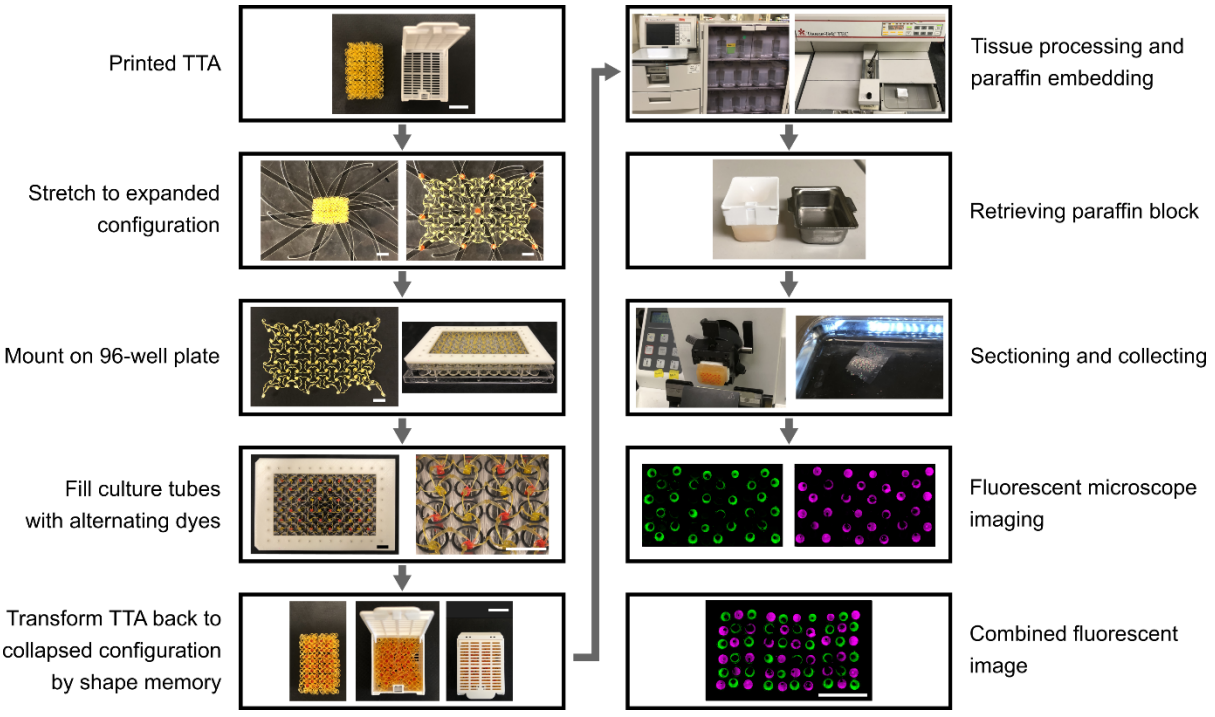

Figure S11. Detailed steps of parallel histological processing. Scale bars are 10 mm

Cell culture materials

B27™, N2™, Gentamicin, GlutaMAX™, fetal bovine serum (FBS), penicillin-streptomycin (PS), 0.05% Trypsin-EDTA, Neurobasal Media™, PrestoBlue® Cell Viability Reagent, MicroAmp™ Optical 96-Well Reaction Plate, MicroAmp™ Optical Adhesive Film, and Dulbecco's Phosphate Buffered Saline (DPBS) were purchased from Thermo Fisher. Heparin sodium salt was purchased from Tocris. bFGF and EGF were purchased from PeproTech. DMEM/F-12, DMEM, Matrigel®, tissue-culture treated plastic (TCP) T25 flasks, 96-well plates, and Ultra-Low Attachment 96-well plates were purchased from Corning. Accutase® was purchased from Innovative Cell Technologies. hNPCs (RenCell®, EMD Millipore) were cultured with 2% B27 ™, 1% GlutaMAX™, 50 μg/ml Gentamicin, 60 μg/ml heparin sodium salt, 20 ng/ml bFGF, 20 ng/ml EGF in DMEM/F-12 proliferation media on Matrigel®-coated tissue culture plastic. Differentiation was initiated by the withdrawal of bFGF and EGF. iPSC-NSC (generous gift from Dr. Muotri, UC San Diego) were cultured in 0.5% B27 ™, 0.5% N2 ™, 20 ng/ml bFGF in 1:1 Neurobasal:DMEM/F-12 proliferation media on Matrigel®-coated tissue culture plastic. C2C12 and HeLa (ATCC) were cultured with 10% FBS, 1% PS in DMEM proliferation media. All cells were maintained in a humified, 37 ºC incubator at 5% CO_2.

Biocompatibility

Cell metabolic assays are commonly used for testing the biocompatibility of materials.[6,7] To verify the biocompatibility of the TTA, we examined cell viability via PrestoBlue™ cell metabolic activity assay. hNPCs and iPSC-NSCs were delaminated and collected via treatment with Accutase®, while C2C12 and HeLa were delaminated and collected via treatment with 0.05% Trypsin-EDTA. Cells were seeded in 200 μL of proliferation media at a density of 5,000 cells per well of a TCP 96-well plate (pretreated with Matrigel®),

n=5 per condition. Media background control wells were prepared without any cells, n=5. After a 20-minute cell-well plate adhesion period, individual culture tubes were added to designated tube viability wells. Cell viability was assessed after 1-day culture using PrestoBlue™ Cell Viability Reagent (Thermo Fisher Scientific) added to tube-containing experimental and no-tube control wells following the manufacturer's suggested protocol. Media aliquots (150 µL per well) were assayed with a plate reader (Tecan infinite 200Pro) for fluorescence (λ_{ex}=560nm, λ_{em}=590nm).

Viability for each cell line was normalized against the corresponding control wells. Across all cell lines examined (i.e. human neural progenitor cells (hNPCs), induced pluripotent stem cell-derived neural stem cells (iPSC-NSCs), C2C12, and HeLa), there was no statistically significant difference in cell viability induced by the TTA as shown in **Figure S12**. The plot shows averaged cell viability with error bars of 1 standard deviation. Excellent cell viability on the TTA was consistently observed across multiple cell lines, suggesting the broad application of the TTA.

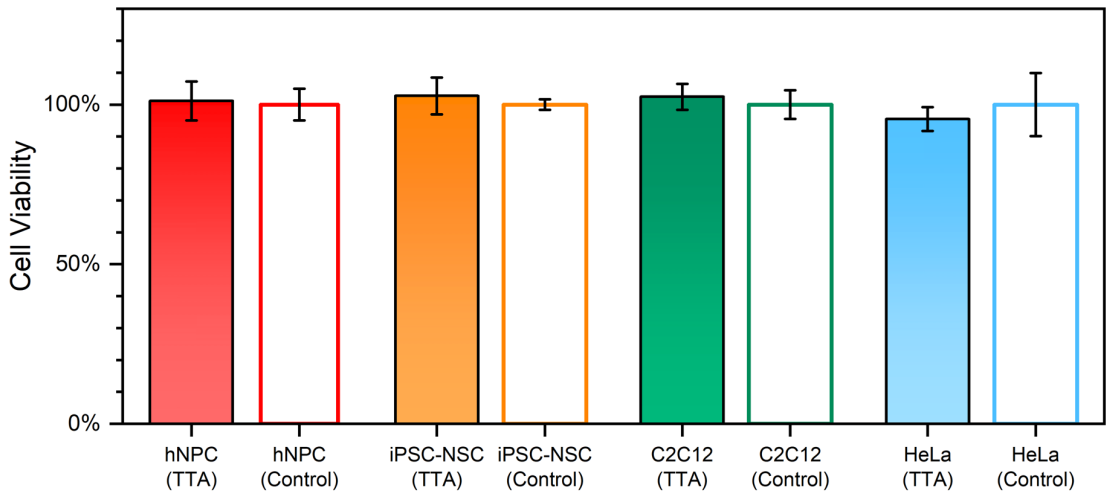

Figure S12. Cell viability of multiple cell lines interacting with the TTA.

Spheroid culture

hNPCs were delaminated and collected via treatment with Accutase® and seeded in 200 µL of proliferation media at a density of 40,000 cells per well of an untreated MicroAmp™ Optical 96-Well Reaction Plate. The cells were cultured overnight covered with MicroAmp™ Optical Adhesive Film to prevent contamination and form initial spheroids. For culturing in a TTA, spheroids in 8 µL media were transferred via pipette into a TTA. The seeded TTA was mounted to a TCP 96-well plate containing 300 µL proliferation or differentiation media. For culturing in a ULA, spheroids in 8 µL media were transferred via pipette to a ULA 96-well plate wells containing 200 µL proliferation or differentiation media. In both cases, daily media changes were performed to compensate for the evaporation of media and to sustain increased metabolic requirements from 3D culture.

Spheroids fixation

The TTA with the cultured spheroids was first transferred to a TCP 96-well plate containing 300 µL DPBS to wash out excess media for 2 minutes, followed by transfer to a TCP 96-well plate containing 300 µL formaldehyde to fix for 20 minutes. Excess formaldehyde in the spheroid-TTA was washed twice with DPBS using the above media washing procedure before storage at 4 ºC. For spheroids in a ULA plate, spheroids were transferred via pipette to a microcentrifuge tube with 1 ml DPBS to wash out excess media for 2 minutes, followed by transfer to a microcentrifuge tube with 1 ml formaldehyde to fix for 20 minutes. Excess formaldehyde was pipetted from the spheroid-containing tube and washed twice with 1 ml DPBS before storage at 4 ºC.

Histology slide preparation

Shape recovery of the TTA (spheroids in TTA only)

The TTA with fixed spheroids was removed from a 96-well plate and heated in an oven at 60 °C for 2 min. After shape recovery, the TTA was placed into a histology cassette (70077-W, Electron Microscopy Sciences) and soaked in 70% ethanol until processing.

Histogel encapsulation (spheroids from the ULA plate only)

Each fixed spheroid in a microcentrifuge tube with DPBS from the previous fixation step was rinsed with 70% ethanol. Ethanol was removed and Histogel (Thermo Fisher) heated to 60 °C was dispensed into the tube to resuspend the spheroid. The tube was then cooled to 4 °C and the solid Histogel plug was removed, sliced into a disc containing the spheroid, and placed in a regular cassette in 70% ethanol.

Processing

Paraffin processing was carried out in an automated processor (Tissue-Tek VIP, Sakura). Samples in the cassette were started in 70% ethanol for 25 min then underwent a series of dehydrations: 2 changes of 95% ethanol, 2 x 25 min, and 3 changes of 100% ethanol, 1 x 15 min, 2 x 25 min. This was followed by 2 x 25 min changes of xylene, and 3 changes of 60 °C melted paraffin: 1 x 15 min, 2 x 25 min (Parapro LMP, StatLab Medical Products).

Embedding

All embedding was performed on an embedding console system (Tissue-Tek TEC, Sakura). For spheroids in the TTA: embedding was following the routine listed prviously and shown in **Figure S8**. For spheroids from the ULA plate: Following processing, the Histogel disc was placed a small shallow base mold (Tissue-Tek 4162, Sakura), which was then filled

with liquid paraffin wax. Before the paraffin wax solidified, the mold was capped with a cassette. After cooling, the paraffin block was demolded and ready for sectioning.

Sectioning and collecting of slides

Paraffin blocks were chilled on ice and then cut at 5µm thickness on a microtome (HM355S, Thermo Scientific). Sections were placed in a 40 ºC water bath, picked up on Platinum Line charged slides (Mercedes Medical), and air-dried.

Deparaffinization

Excess paraffin was melted off slides in a 60 ºC oven for 30 min. Any remaining paraffin was removed in 3 x 3 min changes of xylene. Slides were rehydrated through 2 changes each of 100% and 95% ethanol, then rinsed in water for 1 min.

Estimation of time to prepare Histology slide

Details of estimated time comparison between the ULA plate (conventional method) and the TTA for Histology slide preparation of 60 spheroids are listed in **Table S3**. The upper half of the table was the actual time spent on each step for hNPC neurosphere histology preparation and sectioning. The lower half of the table was the estimated time for preparing 60 spheroids based on the experiment. Shape recovery was only needed for the TTA samples and Histogel Encapsulation was only needed for the ULA plate samples. With steps that could only be done sequentially (i.e. one spheroid at a time), we estimated results as 60 times the duration of their corresponding individual steps. With steps that could be done in parallel, we assumed duration to be identical using both methods.

Table S3. Processing time estimation for 60 spheroids using the ULA plate and the TTA in Histology slide preparation

Per Sample Processing Time (min)		
Shape Recovery	5	
Histogel Encapsulation	30	
Processing	255	
Embedding	ULA plate	TTA
	3	60
Paraffin Wax Solidification	60	
Sectioning	60	
Deparaffinization	50	
60 Spheroids Processing Time (min)		
	ULA plate	TTA
Shape Recovery	N/A	5
Histogel Encapsulation	**30 min x 60 = 1800**	**N/A**
Processing	255	255
Embedding	**3 min x 60 = 180**	**60**
Paraffin Wax Solidification	60	60
Sectioning	**60 min x 60 = 3600**	**60**
Deparaffinization	50	50
Total (min)	5945	490
Total (hour)	**99**	**8.2**

Antigen Retrieval

A homemade antigen retrieval apparatus was used to process deparaffinized slides. Samples are placed in a 10 cm glass Petri dish with 20 ml 0.1M citrate buffer, pH 6. Deionized water is brought to a boil in a glass bowl covered by aluminum foil. A stainless-steel steamer platform is positioned in the antigen retrieval apparatus above the boiling water. The sample-citrate buffer Petri dishes are placed on the platform and allowed to sit in the steamer for 20 minutes followed by a 20-minute cooldown period.

Immunostaining

Bovine serum albumin (BSA), Triton X-100, and FluoroMount ™ were purchased from Sigma Aldrich. Normal goat serum was purchased from Thermo Fisher. The hydrophobic wax pen was purchased from Electron Microscopy Services. Blocking buffer was made with 5% normal goat serum, 0.3% Triton X-100 in DPBS; antibody dilution buffer (ADB) was made with 1% bovine serum albumin, 0.3% Triton X-100 in DPBS. Both buffers were stored at 4 °C until use. Rabbit anti-Tuj1 (Thermo Fisher, cat #PA5-16863), mouse anti-Nestin (Thermo Fisher, cat #MA1-110), goat anti-rabbit AlexaFluor 488 (Thermo Fisher, cat #A-11034), goat anti-mouse AlexaFluor 546 (Thermo Fisher, cat #A-11003) were used at 1:200 dilution. Hoechst 33342 (Thermo Fisher, cat #H3570) was used at 1:100 dilution. Marked, antigen-retrieved samples were treated with a blocking buffer for 1 hour at room temperature. Excess blocking buffer was removed via pipette, and 1° antibody solution (rabbit anti-Tuj1 and mouse anti-Nestin) was treated for 1 hour at room temperature. Stained samples were immersed in DPBS to remove excess antibodies, and 2° antibody solution (goat anti-rabbit 488 and goat anti-mouse 546) was treated for 1.5 hours at room temperature. Fluorescent samples were immersed in DPBS to remove excess antibodies and mounted with FluoroMount™ before storage at -20 °C.

Imaging

Cells were imaged on a Nikon epi-fluorescent microscope using DAPI, FITC, and TRITC filter cubes. Image acquisition parameters were kept consistent throughout all samples. Image processing was performed with ImageJ.

Image processing on Tuj1 stained images for highlighting neural connection

Image processing was performed using MATLAB (The MathWorks Inc. Natick, Massachusetts). To improve visibility of the increased neural connections between cells cultured in differentiation media, we first obtained the magnified fluorescent images from Tuj1 staining (early neural differentiation marker) shown in **Figure 4k to 4n**. The images were converted into 8-bit grayscale (0 to 255) and then binarized with an intensity threshold of 50. The binarized images were then overlaid with 80% transparency on top of the original images. The overlaid images were presented in **Figure S13**.

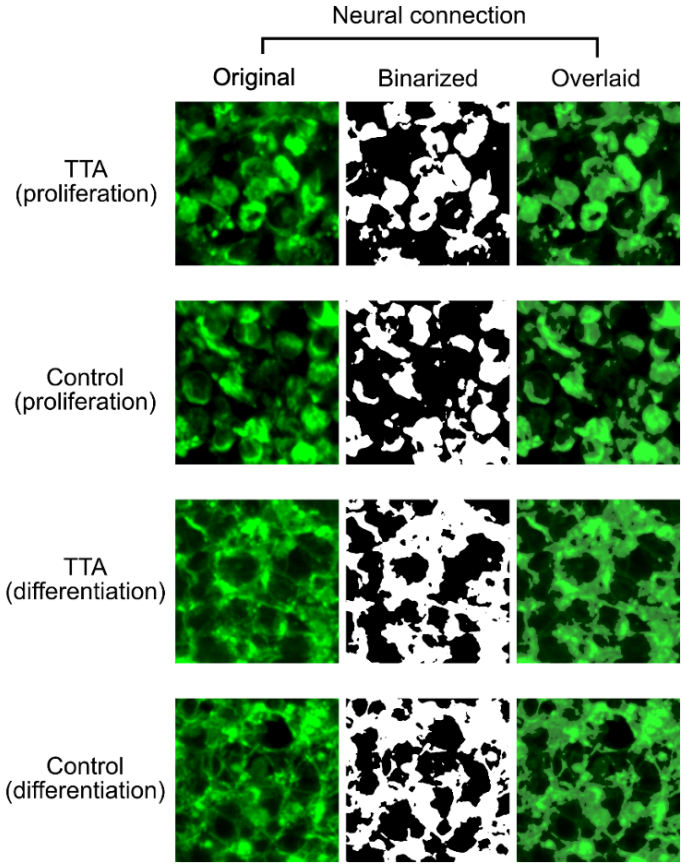

Figure S13. Image processing on Tuj1 stained images to highlight neural connections through binarization and overlaying.

Movie S1. Shape recovery of the TTA at 60 ºC

References for Supporting Information

[1] J. Wu, Z. Zhao, C. M. Hamel, X. Mu, X. Kuang, Z. Guo, H. J. Qi, *Journal of the Mechanics and Physics of Solids* **2018**, *112*, 25.

[2] Q. Ge, A. H. Sakhaei, H. Lee, C. K. Dunn, N. X. Fang, M. L. Dunn, *Scientific Reports* **2016**, *6*, srep31110.

[3] M. Gordon, J. S. Taylor, *Journal of Applied Chemistry* **1952**, *2*, 493.

[4] W. M. Huang, B. Yang, L. An, C. Li, Y. S. Chan, *Appl. Phys. Lett.* **2005**, *86*, 114105.

[5] K. Fan, W. M. Huang, C. C. Wang, Z. Ding, Y. Zhao, H. Purnawali, K. C. Liew, L. X. Zheng, *Express Polym. Lett.* **2011**, *5*, 409.

[6] S. K. Sohaebuddin, P. T. Thevenot, D. Baker, J. W. Eaton, L. Tang, *Part Fibre Toxicol* **2010**, *7*, 22.

[7] A. Kroll, C. Dierker, C. Rommel, D. Hahn, W. Wohlleben, C. Schulze-Isfort, C. Göbbert, M. Voetz, F. Hardinghaus, J. Schnekenburger, *Part Fibre Toxicol* **2011**, *8*, 9.

[8] E. A. Di Marzio, A. J. M. Yang, *J Res Natl Inst Stand Technol* **1997**, *102*, 135.

[9] M. L. Williams, R. F. Landel, J. D. Ferry, *J. Am. Chem. Soc.* **1955**, *77*, 3701.